Gaseous mercury flux from salt marshes is mediated by solar radiation and temperature

Gaseous mercury flux from salt marshes is mediated by solar radiation and temperature

Tom Sizmur[1,2], Gordon McArthur[1,3], David Risk[3], Robert Tordon[4], and Nelson J. O'Driscoll[1]*

[1] Acadia University, Wolfville, Nova Scotia, Canada

[2] University of Reading, Reading, Berkshire, UK

[3] St. Francis Xavier University, Antigonish, Nova Scotia, Canada

[4] Environment Canada, Air Quality Branch, Dartmouth, Nova Scotia

*Department of Earth & Environmental Science, K.C. Irving Environmental Science Center, Acadia University, Wolfville, NS, B4P 2R6, Canada

Abstract

Salt marshes are ecologically sensitive ecosystems where mercury (Hg) methylation and biomagnification can occur. Understanding the mechanisms controlling gaseous Hg flux from salt marshes is important to predict the retention of Hg in coastal wetlands and project the impact of environmental change on the global Hg cycle. We monitored Hg flux from a remote salt marsh over 9 days which included three cloudless days and a 4 mm rainfall event. We observed a cyclical diel relationship between Hg flux and solar radiation. When measurements at the same irradiance intensity are considered, Hg flux was greater in the evening when the sediment was warm than in the morning when the sediment was cool. This is evidence to suggest that both solar radiation and sediment temperature directly influence the rate of Hg(II) photoreduction in salt marshes. Hg flux could be predicted from solar radiation and sediment temperature in sub-datasets collected during cloudless days (R^2 = 0.99), and before (R^2 = 0.97) and after (R^2 = 0.95) the rainfall event, but the combined dataset could not account for the lower Hg flux observed after the rainfall event that is in contrast to greater Hg flux from soils after rainfall events.

Keywords Mercury, Salt marsh, Wetland, Sediment, Dynamic Flux Chamber

Introduction

Mercury (Hg) is a potent neurotoxin that accumulates at the top of aquatic food webs, often far away from emission sources due to long-distance atmospheric transport (Morel et al., 1998). The majority of Hg emitted into the atmosphere is gaseous elemental mercury, Hg(0), which has a residence time of several months in the atmosphere (Corbitt et al., 2011). Although recent efforts to phase out the use of Hg in commercial products has reduced atmospheric emissions (Zhang et al., 2016), anthropogenic sources currently account for only around 30% of emissions (UNEP, 2013). The remainder is attributed to natural sources (10%) and the re-emission of historically emitted anthropogenic sources (60%). The mechanisms underlying the emissions of Hg from ecosystems are imperfectly understood (Agnan et al., 2016). Improving our quantification of these fundamental processes is very important so that we can predict the impact that climate change will have on the global Hg cycle (Krabbenhoft and Sunderland, 2013), and the extent to which Hg will be retained in wetland environments where it can undergo methylation to methylmercury, which is more toxic and biomagnifies through the food web (Gregory Shriver et al., 2006).

Many of the previous attempts to quantify or mechanistically understand gaseous Hg flux from the terrestrial land surface have focussed on soils and freshwater wetlands (Agnan et al., 2016). Relatively little attention has been given to coastal wetlands. Although salt marshes do not represent a large portion of global surface area (they cover a global area of 3.8×10^7 Ha (Steudler and Peterson, 1984) which represents about 0.07% of the total land surface), they are an important Hg sink (Hung and Chmura, 2006). They provide conditions conducive to Hg methylation (Canário et al., 2007) and they support Hg-accumulating invertebrates at the base of sensitive food webs (Sizmur et al., 2013). Salt marshes may become more important sources of Hg flux in the future if more coastal wetlands are created by managed retreat responses to rising sea levels (Sizmur et al., 2016).

The mechanisms controlling Hg flux from coastal sediments is poorly understood since they have only been monitored during two studies (Sommar et al., 2013). Both studies found a positive relationship between Hg flux and solar radiation which indicates that emission of Hg(0) is due to photoreduction of Hg(II) and subsequent volatilisation (Lee et al., 2000; Smith and Reinfelder, 2009).

Lee et al (2000) also found a correlation between Hg flux and sediment temperature, but this relationship is confounded due to the obvious correlation between temperature and solar radiation. Moore and Carpi (2005) suggested that solar radiation mediates Hg(II) reduction to Hg(0) and that temperature mediates the volatilisation of Hg(0) from soils. Pannu et al., (2014) identify a fast, moisture-dependent abiotic process controlling reduction of a small Hg(II) pool, and a concurrent slower biotic process that generates a larger pool of reducible Hg(II) in forest soils. Lindberg et al. (2005; 2002) demonstrate that Hg(0) is volatilised during transpiration of wetland plants. The applicability of these mechanistic insights have not been investigated in coastal wetlands.

There are some key differences between salt marshes and soils or terrestrial wetlands, such as the influence of the tidal cycle, the considerably greater salinity and chloride concentration, and the adaptations of salt marsh vegetation to the anoxic and saline environment. These differences may result in different mechanisms that mediate Hg flux in coastal wetlands when compared to soils or freshwater wetlands. We used a remote, non-point source mercury-contaminated salt marsh on the Bay of Fundy, Nova Scotia, Canada as a model location to investigate Hg flux from coastal wetlands.

Experimental

Study site

The study took place between 6th and 15th July 2009. The study site was located at 45°9'13.61" N, 64°21'30.84"W in a salt marsh near the town of Kingsport on the shores of the Minas Basin of the Bay of Fundy, Nova Scotia, Canada (Figure 1). The Bay of Fundy is well known for its high tidal amplitude and large intertidal zone. The tide height can range >15 m in its upper reaches (Desplanque and Mossman, 2001) with a typical period of 12.4 hours. Because of its proximity to the ocean and the fact it sits close to sea level, the site periodically floods, but was not inundated during the study period. Salt marsh cordgrass (*Spartina alterniflora*) is the dominant plant, while *Spartina pectinata, Salicornia europaea, Cakile edentula* and *Spergularia marina* are also found in the area. The sediment is a red-brown silty clay loam over strongly mottled brown-gray gleyed silty clay loam

derived from red-brown marine sediments. Air temperature during the study had a mean of 16.5°C and reached as high as 27.1°C during the daytime and fell to a minimum of 7.5°C during the nights. Wind speeds averaged 2.6 km hr^{-1} and gusted up to 20.9 km hr^{-1}.

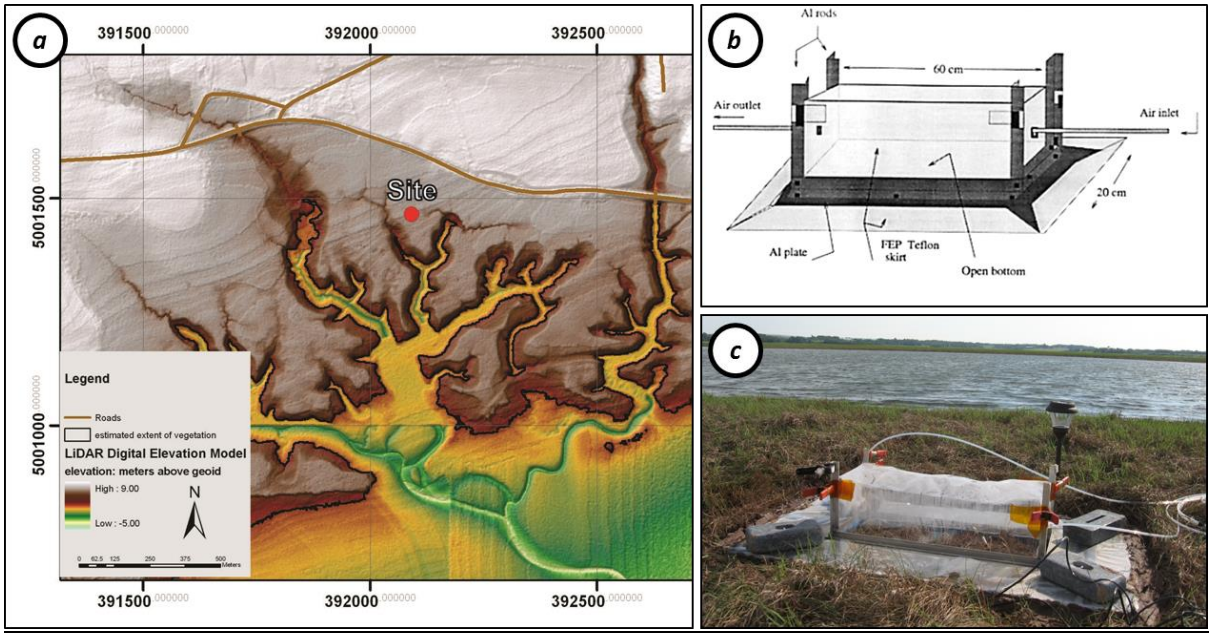

Figure 1 The location of the study site (a) identified on a digital elevation map of the salt marsh near Kingsport, Nova Scotia, in the Minas Basin of the Bay of Fundy. Schematic (b) and photograph (c) of the dynamic Hg flux chamber used to measure Hg flux at the site continuously over a 9-day period.

Sediment sampling and total mercury analysis

Two 30 cm sediment cores were sampled at the site using a polypropylene hand corer and transported to the lab for sectioning. Core sections were separated into mineral and vegetation components in >18.2 MΩ water and dried for 72 hours in a drying oven at 40°C. Dried samples were homogenized with a mortar and pestle and all equipment was cleaned between samples using water and trace grade ethanol. Vegetation samples were flash frozen with liquid nitrogen to aid in the homogenization process. Wet and dry mass of samples were recorded and total mercury in samples was determined by thermal degradation of samples and gold amalgamation atomic absorbance analysis using a Nippon MA-2000.

98

99 Dynamic Hg Flux Chamber Technique

100 Gaseous Hg flux was measured every 10 minutes over the 9-day study period from 6th to 15th July
101 2009 using a dynamic flux chamber technique based on the method described by Carpi and Lindberg
102 (Carpi and Lindberg, 1997). A Durafilm© chamber (20 cm H x 20 cm W x 60 cm L), covering an
103 area 0.12 m^2 and made of 5 mil Teflon, was set on the sediment surface (Figure 1). Through an inlet
104 and outlet at either end of the chamber ambient air was pumped through the chamber at a constant rate
105 of 1.5 dm^3 min^{-1}, following Agnan et al.(2016). Dead air periods in the chamber were avoided by
106 using a Tekran switching controller and second pump with a mass flow controller.

107 Mercury concentration at the inlet of the chamber reports the ambient concentration, while the
108 mercury concentration at the outlet reports the chamber concentration. The inlet and outlet Hg
109 concentrations were measured and compared using a dual channel Tekran Model 2537 mercury
110 analyzer and used to calculate Hg flux (ng m^{-2} h^{-1}) from the dynamic chamber using the equation:

111 $$\text{Hg flux} = \frac{[\text{Hg}]\text{o} - [\text{Hg}]\text{i}}{\text{A}} \times \text{Q}$$

112 Where [Hg]o is the Hg concentration (ng m^{-3}) of air measured at the outlet, [Hg]i is the Hg
113 concentration (ng m^{-3}) at the inlet, A denotes the area (0.12 m^2) of the bottom of the chamber in
114 contact with the system measured and Q is the flow rate (1.5 dm^3 min^{-1}) of air through the chamber.

115 The dual channel Tekran analyser sampled two successive 5 minute air samples from the chamber
116 inlet, followed by two successive 5 minute air samples flowing from the chamber outlet, ensuring that
117 both gold cartridges were used for measuring both inlet and outlet air and any degradation of trap
118 recoveries could be easily identified. Subsequently the flux was measured every 10 minutes. The time
119 required to completely recycle the air in the chamber was about 16 minutes.

120 Prior to deploying the chamber at the study site the chamber system was tested for recovery of Hg(0)
121 using standard injections from a Tekran 2505 mercury vapour external calibration unit and a Hamilton
122 digital syringe. Recovery rates of Hg(0) injected into the chamber were consistently >90%.

Recoveries were also tested via manual injections in the field every 48 hours with similar recoveries (>90%). As such data were not recovery corrected. Chamber blanks were also measured over a clean Teflon sheet using mercury free air. The level of mercury measured in the mercury-free gas and chamber air was below the detection limit of 0.01ng m^{-3}. Field measurements less than 0.01 ng m^{-3} were treated as nondetectable (0 readings) in the dataset.

Meteorological Sensors

A Davis weather station recorded relative humidity, air temperature, wind speed, solar radiation and barometric pressure at the study site. In addition, Campbell Scientific 107b thermistors were installed to measure temperature of (i) the sediment 4 cm underneath the flux chamber, (ii) the air inside the flux chamber, and (iii) the air outside the chamber every 5 minutes and coupled to a Campbell Scientific CR1000 datalogger.

The intensity and spectral distribution of incoming solar radiation was quantified using an OceanOptics USB 4000 spectroradiometer with a fibre-optic (10 m length, 200 um diameter) and spectral diffusion probe (diameter 4.3 mm). The spectroradiometer probe was fastened to the outside of the frame supporting the mercury flux chamber approximately 20 cm above the ground surface. Based on controlled measurements in the lab, there is <12% loss of UV radiation (280-400 nm) through the flux chamber Teflon film. Spectral readings were taken continuously every 5 minutes during the field campaign for UVA (280-320 nm), UVB (320-400 nm), visible (400-800 nm), and total UV-visible radiation (280-800 nm) and integrated using spectra suite software.

Because meteorological measurements were taken every 5 minutes and Hg flux only calculated every 10 minutes, Hg flux measurements were matched to the average of two sequentially collected meteorological measurements.

148 **Results and discussion**

149 Concentration of total Hg in the sediments

150 The concentration of total Hg in the sediments ranged between 1.6 and 22.1 ng g^{-1} in the top 35 cm of
151 the mineral sediments (Figure 2), peaking at a depth of 12 cm. Concentrations in the root biomass
152 were considerably higher, ranging between 39.0 and 223.4 ng g^{-1} and showing a similar depth profile
153 to the mineral sediment (Figure 1). Sediment Hg concentrations (Figure 1) were within the range of
154 previous wetland and mudflat observations in the Minas Basin of the Bay of Fundy (O'Driscoll et al.,
155 2011; Sizmur et al., 2013) but considerably lower than salt marsh sites affected by local point-source
156 pollution (Canário et al., 2010; Mitchell and Gilmour, 2008).

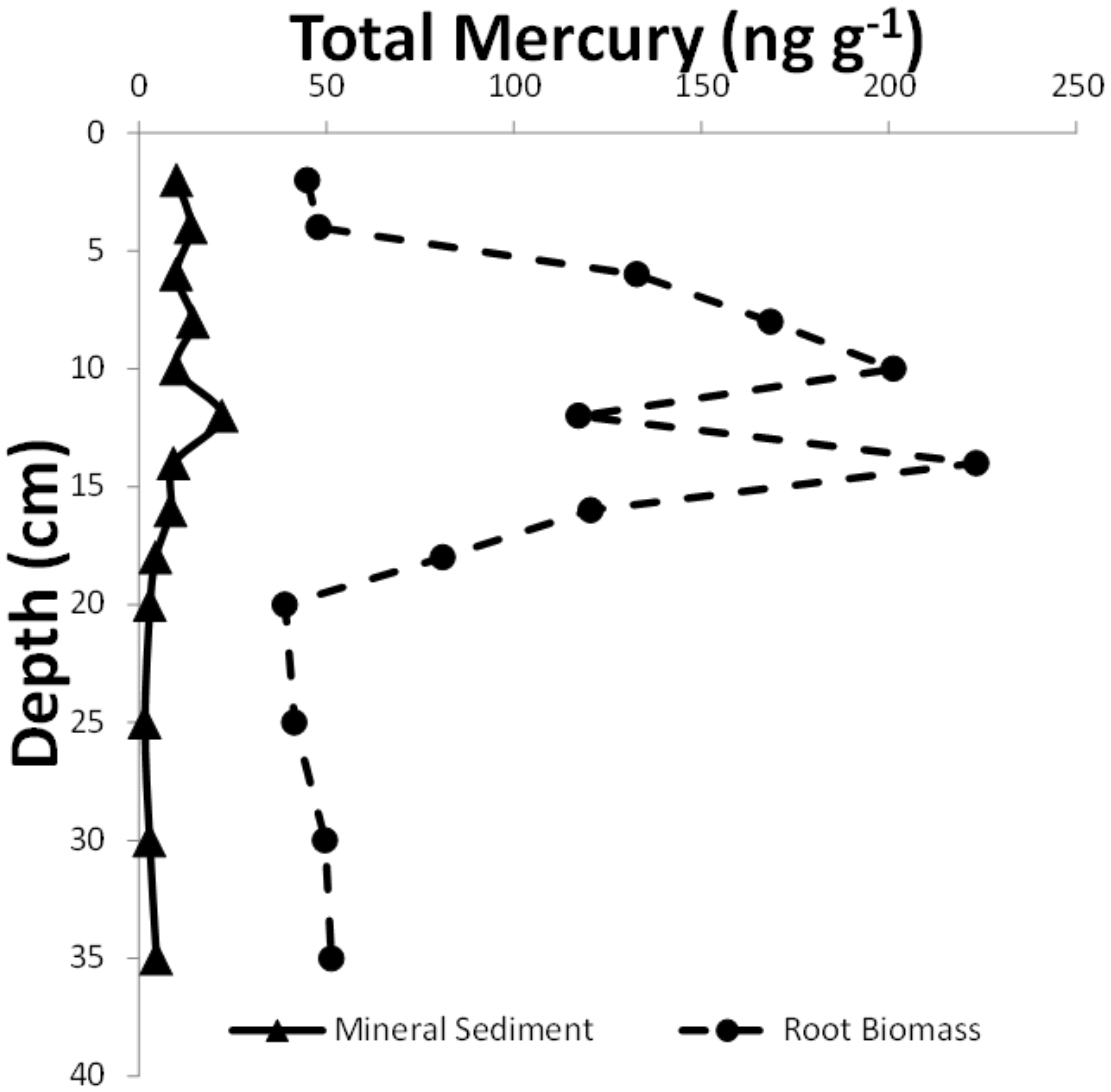

157

158 Figure 2 Total mercury concentration with depth in mineral sediments and root biomass at the site.

159 Gaseous Hg flux measurements from salt marshes

160 The Hg flux ranged -0.61 to 4.83 ng m^{-2} hr^{-1} during the course of the 9-day monitoring period with an
161 overall mean of 1.17 ng m^{-2} hr^{-1} (Figure 3). These fluxes are an order of magnitude lower than those
162 observed from the Great Bay estuary (mean 17 ng m^{-2} hr^{-1}), a non-point source mercury-contaminated
163 (450 ng g^{-1}) salt marsh in New Jersey (Smith and Reinfelder, 2009). The negative values we observed
164 (18.4% of total observations) occurred during the night time and are thought to have been due to Hg
165 deposition. In contrast, Lee et al. (2000) observed negative flux during the daytime and an overall
166 negative flux (mean -3.3 ng m^{-2} hr^{-1}) at a non-point source mercury-contaminated (200-470 ng g^{-1}) salt
167 marsh in Connecticut during a similar period of the year (Day 180-200 in 1998). Both studies
168 described above were conducted at sites that, despite being non-point source mercury-contaminated,
169 had sediment Hg concentrations (450 ng g^{-1} and 200-470 ng g^{-1}) more than an order of magnitude
170 greater than our site (1.6-22 ng g^{-1}; Figure 2). Both studies also used the micrometeorological method
171 to measure Hg flux (Sommar et al., 2013).

172 Our study used the dynamic flux chamber method to monitor Hg flux from a salt marsh. The
173 temperature in the dynamic flux chamber is usually greater than the ambient air temperature and so
174 often results in the measurement of artificially higher fluxes than the micrometeorological method
175 (Agnan et al., 2016) but can exhibit lower concentrations due to the absence of turbulence (Zhu et al.,
176 2015b). Zhu et al (2015b) found that dynamic flux chamber measurements lagged 2 hours behind Hg
177 flux measured using the micrometeorological methods and exhibited a positive bias in the afternoon
178 due to the changes in soil temperature lagging behind air temperature (Zhu et al., 2015a). However,
179 the dynamic flux chamber offers a greater capability to link the environmental conditions in and under
180 the specific chamber area to the Hg flux observed (especially in heterogeneous environments or in
181 coastal zones where wind direction changes diurnally).

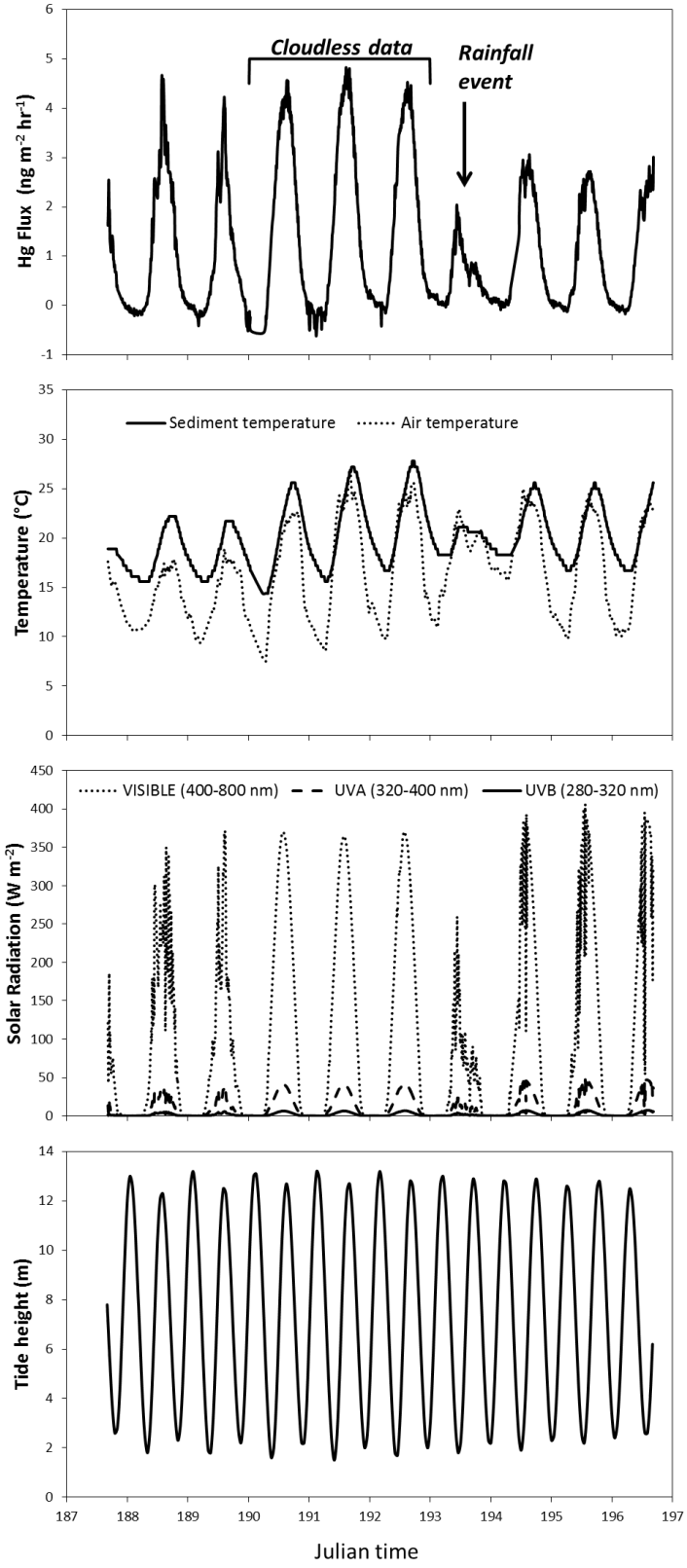

Figure 3 Time course data of gaseous Hg flux from the sediment, temperature of the sediment and the ambient air, incoming solar radiation (in the visible, UVA and UVB spectrum), and tidal height during the course of a continuous 9-day monitoring period from 6th to 15th July 2009 on a salt marsh near Kingsport, Nova Scotia, in the Minas Basin of the Bay of Fundy. Three cloudless days (8th to 11th) and a 4 mm rainfall event (at 2pm on the 12th) are identified on the Hg flux plot.

During the course of the 9-day continuous monitoring of Hg flux from the salt marsh, there were three cloudless days, from 8th to 11th July 2009 (Figure 3), which exposed the chamber to three diurnal cycles of direct sunlight without interruption. There was also a 4mm rainfall event from 14:00 to 15:30 on 12th July (Figure 3) which suppressed the Hg flux thereafter. To aid our interpretation of the data we analysed our dataset as four sub-datasets:

- All data (17:17 on 6th July to 15:27 on 15th July, n = 1212)
- Pre-rain data (17:17 on 6th July to 13:47 on 12th July, n = 789)
- Post rain data (13:57 on 12th July to 15:27 on 15th July, n = 422)
- Cloudless data (23:57 on 8th July to 23:57 on 11th July, n = 393)

Hysteresis between solar radiation and Hg flux can be explained by sediment temperature

There was a clear diurnal fluctuation in Hg flux, which peaked during the middle of the day at the same time as the peak in solar radiation and air temperature (Figure 3). We found a positive relationship between solar radiation (280-800 nm) and Hg flux (Figure 4), in agreement with several other authors finding positive correlations at sites on grassland soils (Obrist et al., 2005), forest soils (Choi and Holsen, 2009), oceans (Fantozzi et al., 2007), freshwater lakes (O'Driscoll et al., 2003), snow (Mann et al., 2015), and salt marshes (Lee et al., 2000; Smith and Reinfelder, 2009). These observations support the hypothesis that Hg flux is driven by photochemical reduction of Hg(II) to Hg(0) and subsequent volatilisation of Hg(0) from the sediment. Because the intensity of solar radiation at each waveband (UVA, UVB and visible) co-correlated, we could not elucidate which wavelength was primarily responsible for stimulating the photochemical reactions.

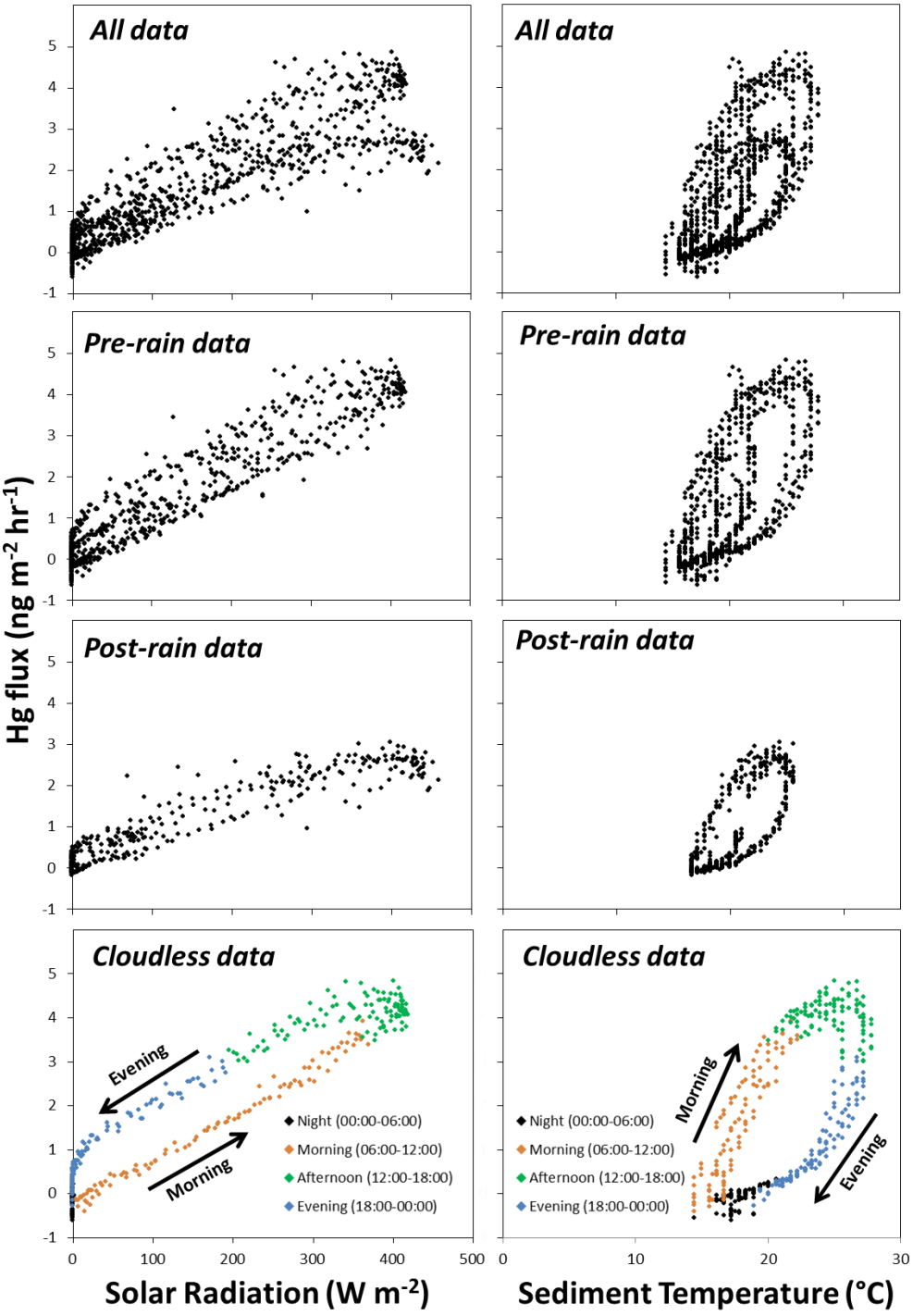

209

210 Figure 4 Gaseous Hg flux data from a salt marsh over a 9-day period plotted against the total
211 incoming solar radiation in the range 280-800 nm and the temperature of the underlying sediment at a
212 depth of 4 cm. All the data (from 6th to 15th July 2009) is presented in the top plot above the data
213 collected before and after a 4 mm rainfall event (at 2pm on the 12th) are presented separately. Data
214 collected during three cloudless days (8th to 11th) before the rainfall event is presented at the bottom
215 and divided into measurements made during the night (00:00-06:00), morning (06:00-12:00),
216 afternoon (12:00-18:00), and evening (18:00-00:00). There is a clear hysteresis in the data (observed
217 most clearly in the cloudless dataset) as Hg flux is greater during the evening when the sediment is
218 warm than in the morning when sediment is cool.

We found a clear cyclical diel relationship between solar radiation and Hg flux (Figure 4) which can most easily be identified when plotting the data collected during three cloudless days from 8th to 11th July 2009. At the same irradiance intensity, Hg flux is greater in the evening (18:00-00:00) than the morning (06:00-12:00.) A similar relationship was found in morning and afternoon Hg flux measurements made from coastal seawater (Lanzillotta and Ferrara, 2001). This cyclical relationship, also referred to as hysteresis, can result from a time-lag between a controlling variable and its measured effect, such as the delayed response of soil respiration to increasing temperature (Phillips et al., 2011). However, it can also be a result of the simultaneous influence of several confounding variables, such as solar radiation and temperature.

Several authors have observed positive correlations between Hg flux and air or soil temperature as well as solar radiation (Lee et al., 2000; Lindberg et al., 1999; Obrist et al., 2005), and some note a closer relationship between temperature and Hg flux than between solar radiation and Hg flux (Gillis and Miller, 2000; Ma et al., 2013). However, these measurements confound one another since an increase in incipient radiation causes an increase in temperature. In our study we did not find a satisfactory correlation between Hg flux and either solar radiation, air temperature or sediment temperature singularly since all three relationships result in a cyclical relationship (hysteresis) that is most easily observed in the dataset collected on the cloudless days (Figure SI-1). Multiple linear regression models fit using only solar radiation and sediment temperature as the explanatory variables demonstrate that these two variables together can predict Hg flux in our sub-datasets with a high degree of certainty (Figure 5). The models significantly ($p<0.001$) predict Hg flux using the pre-rain dataset ($R^2 = 0.97$), the post-rain dataset ($R^2 = 0.95$) and the cloudless dataset ($R^2 = 0.99$). When measurements at the same irradiance intensity are considered, Hg flux is greater in the evening (18:00-00:00) when the salt marsh is warmer than in the morning (06:00-12:00) when the marsh is cooler (Figure 4). The cyclical relationship between solar radiation and Hg flux can therefore be explained by differences in the temperature of the sediment in the morning compared to the evening, supported by Zhu et al (2015b) who observe Hg flux peaking in in concert with soil temperature.

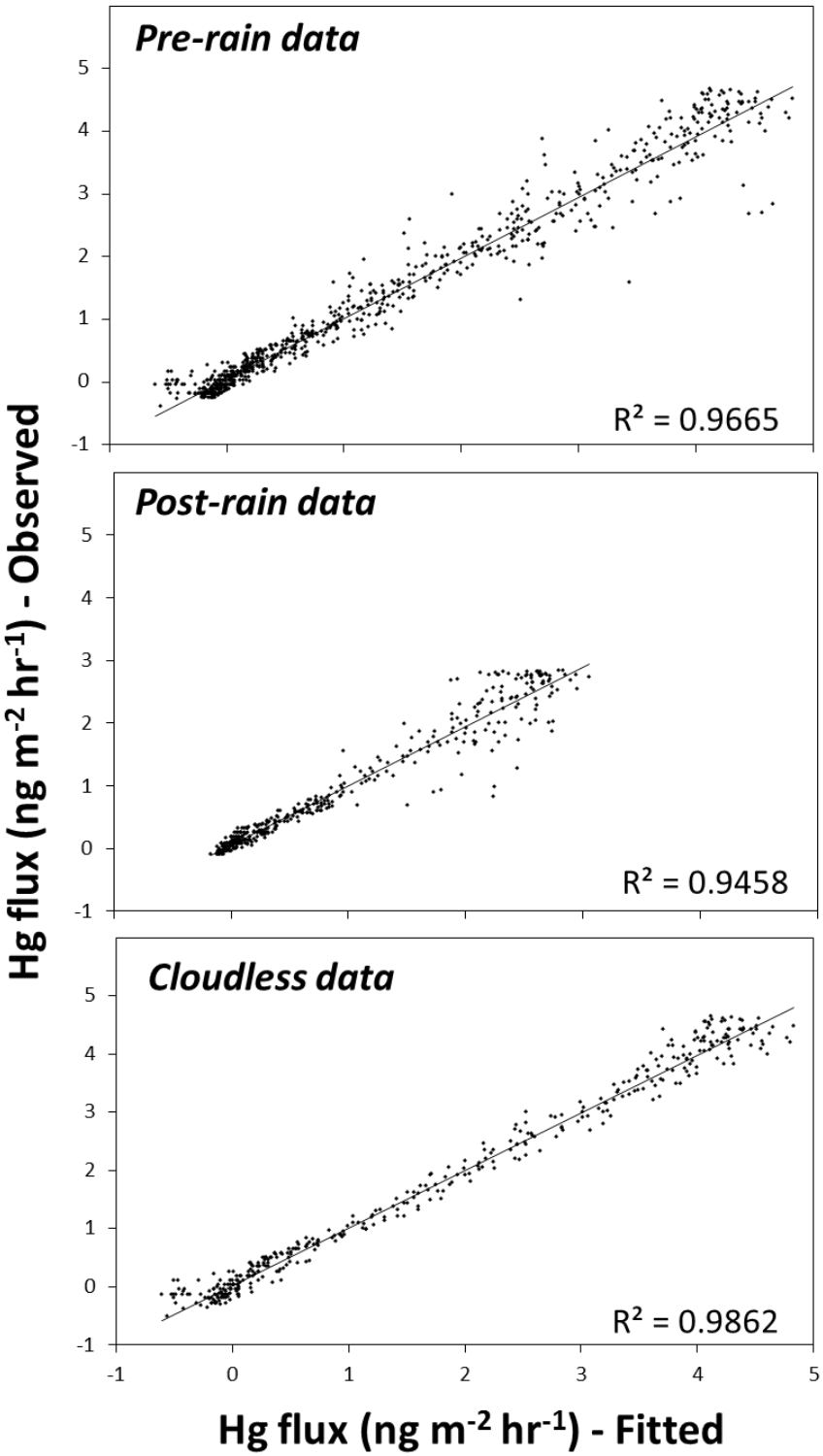

246

247 Figure 5 Gaseous Hg flux from a salt marsh before a 4 mm rainfall event (6th to 12th July 2009), after
248 the rainfall event (12th to 15th), and during three cloudless days (8th to 11th) before the rainfall event
249 plotted against fitted fluxes predicted using multiple linear regression models created with the same
250 data. The models use solar radiation (280-800nm) and sediment temperature below the flux chamber
251 and as explanatory variables.

252

There is uncertainty in the literature concerning whether temperature affects Hg flux by indirectly increasing the proportion of Hg(II) that is available for photoreduction or whether it directly affects Hg flux by providing energy for Hg(0) volatilization from soils (Bahlmann et al., 2006; Moore and Carpi, 2005). Based on our observations, we advance the hypothesis that sediment temperature has an indirect effect on Hg flux by directly influencing the rate of Hg(II) photoreduction, but not directly influencing volatilization which may be due to abiotic desorption (Moore and Carpi, 2005), or the result of transpiration by the salt marsh vegetation (Lindberg et al., 2002). Our hysteresis graphs show that the direction of the cyclical relationship between sediment temperature and Hg flux occurs in the opposite direction to the relationship between solar radiation and Hg flux (Figure 4). When measurements at the same temperature are considered, Hg flux is greater in the morning (06:00-12:00), when the solar radiation is higher, than the evening (18:00-12:00) when the solar radiation is lower. If temperature has a direct effect on Hg flux by providing energy for desorption of Hg(0) from sediment surfaces and subsequent volatilization from the soil then we would expect to see a weak relationship between solar radiation and Hg flux in the evening because build-up of Hg(0) during the day would continue to be emitted from the relatively warm sediment during the evening. Instead, it seems that both solar radiation and sediment temperature are influencing the same rate-limiting process responsible for Hg flux.

Rainfall supresses Hg flux from salt marshes

We observed lower Hg flux after a 4 mm 90 minute rainfall event on 12th July 2009 but an otherwise similar cyclical relationship between solar radiation and Hg emissions (Figure 4) that can be explained by the sediment being cool in the morning and warm in the evening (Figure 5). Our observations contrast with several papers describing an immediate pulse of Hg released after rainfall events due to a moisture-dependent displacement of Hg(0)-containing air from pores followed by a greater rate of Hg flux from bare soil (Song and Van Heyst, 2005), desert soils (Lindberg et al., 1999), agricultural soils (Briggs and Gustin, 2013), and floodplain soils (Wallschläger et al., 2000).

A key difference between the salt marsh where we made our observations and the soils monitored in the abovementioned studies is that the salt marsh is tidally influenced. We hypothesised that the incoming tide would cause displacement of Hg(0)-containing air from the sediment and provide a clear influence of the tidal cycle on Hg flux. However, as observed by Smith and Reinfelder (2009) and Lee et al (2000), we found no relationship between the tidal cycle and Hg flux. The rainfall event occurred during an incoming tide and also did not result in a pulse of Hg flux. Therefore, displacement of Hg(0)-containing air from sediment does not seem to contribute to Hg flux in salt marshes, probably because the frequent movement of air in the salt marsh sediment (due to the tidal cycle) does not allow Hg(0)-containing air to build up in the pores.

Rinklebe et al., (2010) demonstrate a negative correlation between soil water content and Hg flux in a seasonally flooded terrestrial wetland, since the soils are generally wetter during the winter when temperature and solar radiation are lower. However, in laboratory incubations, at constant temperature, they reveal greater flux from wet or saturated soils compared to dry soils 24 and 48 hours after artificial wetting. These observations are further supported by data from Pannu et al., (2014) indicating that Hg flux from soils increases with increasing water-filled pore space (WFPS) and peaked at 60% WFPS. However, this study also showed that increasing moisture to 80% WFPS the Hg flux was considerably suppressed. Briggs and Gustin (2013) also note that after the initial pulse following a rainfall event, the Hg flux can become supressed if the soil is saturated with water. This suppression is due to a slower diffusivity of Hg(0) through water-filled pores as opposed to through air-filled pores. In our experiment it is possible that some of the pores in the sediment became saturated after the rainfall event and that slower diffusivity of Hg(0) is the reason for the suppressed Hg flux. If transpiration of Hg(0) by wetland vegetation is a major mechanism controlling Hg flux from the sediment (Lindberg et al., 2002) then the observed decrease in Hg flux may have been due to stomatal closure and a subsequent decrease in the rate of transpiration under saturated conditions (Pezeshki and DeLaune, 2012; Pezeshki, 2001).

Environmental significance

We provide here 9 days of continuous Hg flux measurements made on a salt marsh using the Dynamic Flux Chamber technique. Because the Hg flux measurements made can be directly related to the sediment underneath the chamber we elucidate an important diurnal mechanism that has not been previously identified. Our data supports the hypothesis that photoreduction of Hg(II) to Hg(0) is mediated by both sediment temperature and solar radiation and that photoreduction (rather than volatilisation of Hg(0)) is the rate limiting step in these sediments. This mechanistic insight reduces the uncertainty concerning the role of solar radiation and temperature in Hg flux from terrestrial surfaces. We also present data to suggest that the impact of rainfall on Hg flux behaves differently at coastal sites compared to terrestrial wetlands or soils. Here we show that Hg flux is suppressed after a rainfall event, possibly due to lower transpiration by salt marsh vegetation. The measurements of Hg flux and insights into the mechanisms controlling Hg flux presented here increase our knowledge of the global mercury cycle and provide a mechanistic framework for integrating coastal wetlands into global Hg flux models. However, caution should be exercised when applying this data for modelling since Hg flux is highly variable both spatially and temporally (During et al., 2009).

Acknowledgements

This research was supported by an NSERC discovery grant (#341960-2008) and Canada Research Chair grant (#950-203477) to N.O. Field and technical support was provided by John Dalziel.

References

Agnan, Y., Le Dantec, T., Moore, C.W., Edwards, G.C., Obrist, D., 2016. New Constraints on Terrestrial Surface–Atmosphere Fluxes of Gaseous Elemental Mercury Using a Global Database. Environmental Science & Technology 50, 507-524. 10.1021/acs.est.5b04013

Bahlmann, E., Ebinghaus, R., Ruck, W., 2006. Development and application of a laboratory flux measurement system (LFMS) for the investigation of the kinetics of mercury emissions from soils. Journal of Environmental Management 81, 114-125. 10.1016/j.jenvman.2005.09.022

Briggs, C., Gustin, M.S., 2013. Building upon the Conceptual Model for Soil Mercury Flux: Evidence of a Link Between Moisture Evaporation and Hg Evasion. Water, Air, & Soil Pollution 224, 1-13. 10.1007/s11270-013-1744-5

Canário, J., Caetano, M., Vale, C., Cesário, R., 2007. Evidence for Elevated Production of Methylmercury in Salt Marshes. Environmental Science & Technology 41, 7376-7382. 10.1021/es071078j

Canário, J., Vale, C., Poissant, L., Nogueira, M., Pilote, M., Branco, V., 2010. Mercury in sediments and vegetation in a moderately contaminated salt marsh (Tagus Estuary, Portugal). Journal of Environmental Sciences 22, 1151-1157. 10.1016/S1001-0742(09)60231-X

Carpi, A., Lindberg, S.E., 1997. Sunlight-mediated emission of elemental mercury from soil amended with municipal sewage sludge. Environmental Science & Technology 31, 2085-2091. 10.1021/es960910+

Choi, H.-D., Holsen, T.M., 2009. Gaseous mercury fluxes from the forest floor of the Adirondacks. Environmental Pollution 157, 592-600. 10.1016/j.envpol.2008.08.020

Corbitt, E.S., Jacob, D.J., Holmes, C.D., Streets, D.G., Sunderland, E.M., 2011. Global source–receptor relationships for mercury deposition under present-day and 2050 emissions scenarios. Environmental Science & Technology 45, 10477-10484. 10.1021/es202496y

Desplanque, C., Mossman, D.J., 2001. Bay of Fundy tides. Geoscience Canada 28

During, A., Rinklebe, J., Böhme, F., Wennrich, R., Stärk, H.-J., Mothes, S., Du Laing, G., Schulz, E., Neue, H.-U., 2009. Mercury volatilization from three floodplain soils at the Central Elbe River, Germany. Soil and Sediment Contamination 18, 429-444. 10.1080/15320380902962395

Fantozzi, L., Ferrara, R., Frontini, F.P., Dini, F., 2007. Factors influencing the daily behaviour of dissolved gaseous mercury concentration in the Mediterranean Sea. Marine Chemistry 107, 4-12. 10.1016/j.marchem.2007.02.008

Gillis, A.A., Miller, D.R., 2000. Some local environmental effects on mercury emission and absorption at a soil surface. Science of The Total Environment 260, 191-200. 10.1016/S0048-9697(00)00563-5

Gregory Shriver, W., Evers, D.C., Hodgman, T.P., MacCulloch, B.J., Taylor, R.J., 2006. Mercury in sharp-tailed sparrows breeding in coastal wetlands. Environmental Bioindicators 1, 129-135. 10.1080/15555270600695734

Hung, G.A., Chmura, G.L., 2006. Mercury accumulation in surface sediments of salt marshes of the Bay of Fundy. Environmental Pollution 142, 418-431. 10.1016/j.envpol.2005.10.044

Krabbenhoft, D.P., Sunderland, E.M., 2013. Global change and mercury. Science 341, 1457-1458. 10.1126/science.1242838

Lanzillotta, E., Ferrara, R., 2001. Daily trend of dissolved gaseous mercury concentration in coastal seawater of the Mediterranean basin. Chemosphere 45, 935-940. 10.1016/S0045-6535(01)00021-2

Lee, X., Benoit, G., Hu, X., 2000. Total gaseous mercury concentration and flux over a coastal saltmarsh vegetation in Connecticut, USA. Atmospheric Environment 34, 4205-4213. 10.1016/S1352-2310(99)00487-2

Lindberg, S., Zhang, H., Gustin, M., Vette, A., Marsik, F., Owens, J., Casimir, A., Ebinghaus, R., Edwards, G., Fitzgerald, C., 1999. Increases in mercury emissions from desert soils in response to rainfall and irrigation. Journal of Geophysical Research: Atmospheres 104, 21879-21888. 10.1029/1999JD900202

Lindberg, S.E., Dong, W., Chanton, J., Qualls, R.G., Meyers, T., 2005. A mechanism for bimodal emission of gaseous mercury from aquatic macrophytes. Atmospheric Environment 39, 1289-1301. 10.1016/j.atmosenv.2004.11.006

Lindberg, S.E., Dong, W., Meyers, T., 2002. Transpiration of gaseous elemental mercury through vegetation in a subtropical wetland in Florida. Atmospheric Environment 36, 5207-5219. 10.1016/S1352-2310(02)00586-1

Ma, M., Wang, D., Sun, R., Shen, Y., Huang, L., 2013. Gaseous mercury emissions from subtropical forested and open field soils in a national nature reserve, southwest China. Atmospheric Environment 64, 116-123. 10.1016/j.atmosenv.2012.09.038

Mann, E.A., Mallory, M.L., Ziegler, S.E., Avery, T.S., Tordon, R., O'Driscoll, N.J., 2015. Photoreducible Mercury Loss from Arctic Snow Is Influenced by Temperature and Snow Age. Environmental Science & Technology 49, 12120-12126. 10.1021/acs.est.5b01589

Mitchell, C.P., Gilmour, C.C., 2008. Methylmercury production in a Chesapeake Bay salt marsh. Journal of Geophysical Research: Biogeosciences 113. 10.1029/2008JG000765

Moore, C., Carpi, A., 2005. Mechanisms of the emission of mercury from soil: Role of UV radiation. Journal of Geophysical Research: Atmospheres 110. 10.1029/2004JD005567

Morel, F.M., Kraepiel, A.M., Amyot, M., 1998. The chemical cycle and bioaccumulation of mercury. Annual review of ecology and systematics, 543-566. www.jstor.org/stable/221718

O'Driscoll, N.J., Beauchamp, S., Siciliano, S.D., Rencz, A.N., Lean, D.R.S., 2003. Continuous Analysis of Dissolved Gaseous Mercury (DGM) and Mercury Flux in Two Freshwater Lakes in Kejimkujik Park, Nova Scotia: Evaluating Mercury Flux Models with Quantitative Data. Environmental Science & Technology 37, 2226-2235. 10.1021/es025944y

O'Driscoll, N.J., Canário, J., Crowell, N., Webster, T., 2011. Mercury speciation and distribution in coastal wetlands and tidal mudflats: relationships with sulphur speciation and organic carbon. Water, Air, & Soil Pollution 220, 313-326. 10.1007/s11270-011-0756-2

Obrist, D., Gustin, M.S., Arnone Iii, J.A., Johnson, D.W., Schorran, D.E., Verburg, P.S.J., 2005. Measurements of gaseous elemental mercury fluxes over intact tallgrass prairie monoliths during one full year. Atmospheric Environment 39, 957-965. 10.1016/j.atmosenv.2004.09.081

Pannu, R., Siciliano, S.D., O'Driscoll, N.J., 2014. Quantifying the effects of soil temperature, moisture and sterilization on elemental mercury formation in boreal soils. Environmental Pollution 193, 138-146. 10.1016/j.envpol.2014.06.023

Pezeshki, S., DeLaune, R., 2012. Soil oxidation-reduction in wetlands and its impact on plant functioning. Biology 1, 196-221. 10.3390/biology1020196

Pezeshki, S.R., 2001. Wetland plant responses to soil flooding. Environmental and Experimental Botany 46, 299-312. 10.1016/S0098-8472(01)00107-1

Phillips, C.L., Nickerson, N., Risk, D., Bond, B.J., 2011. Interpreting diel hysteresis between soil respiration and temperature. Global Change Biology 17, 515-527. 10.1111/j.1365-2486.2010.02250.x

Rinklebe, J., During, A., Overesch, M., Du Laing, G., Wennrich, R., Stärk, H.-J., Mothes, S., 2010. Dynamics of mercury fluxes and their controlling factors in large Hg-polluted floodplain areas. Environmental Pollution 158, 308-318. 10.1016/j.envpol.2009.07.001

Sizmur, T., Canário, J., Gerwing, T.G., Mallory, M.L., O'Driscoll, N.J., 2013. Mercury and methylmercury bioaccumulation by polychaete worms is governed by both feeding ecology and mercury bioavailability in coastal mudflats. Environmental Pollution 176, 18-25. 10.1016/j.envpol.2013.01.008

Sizmur, T., Godfrey, A., O'Driscoll, N.J., 2016. Effects of coastal managed retreat on mercury biogeochemistry. Environmental Pollution 209, 99-106. 10.1016/j.envpol.2015.11.016

Smith, L.M., Reinfelder, J.R., 2009. Mercury volatilization from salt marsh sediments. Journal of Geophysical Research: Biogeosciences 114. 10.1029/2009JG000979

Sommar, J., Zhu, W., Lin, C.-J., Feng, X., 2013. Field Approaches to Measure Hg Exchange Between Natural Surfaces and the Atmosphere—A Review. Critical Reviews in Environmental Science and Technology 43, 1657-1739. 10.1080/10643389.2012.671733

Song, X., Van Heyst, B., 2005. Volatilization of mercury from soils in response to simulated precipitation. Atmospheric Environment 39, 7494-7505. 10.1016/j.atmosenv.2005.07.064

Steudler, P.A., Peterson, B.J., 1984. Contribution of gaseous sulphur from salt marshes to the global sulphur cycle. Nature 311, 455-457. 10.1038/311455a0

UNEP, U., 2013. Global Mercury Assessment 2013: Sources, Emissions, Releases and Environmental Transport. United Nations Environment Programme Chemicals Branch, Geneva, Switzerland.

Wallschläger, D., Herbert Kock, H., Schroeder, W.H., Lindberg, S.E., Ebinghaus, R., Wilken, R.-D., 2000. Mechanism and significance of mercury volatilization from contaminated floodplains of the German river Elbe. Atmospheric Environment 34, 3745-3755. 10.1016/S1352-2310(00)00083-2

Zhang, Y., Jacob, D.J., Horowitz, H.M., Chen, L., Amos, H.M., Krabbenhoft, D.P., Slemr, F., St. Louis, V.L., Sunderland, E.M., 2016. Observed decrease in atmospheric mercury explained by global

436 decline in anthropogenic emissions. Proceedings of the National Academy of Sciences 113, 526-531.
437 10.1073/pnas.1516312113

438 Zhu, W., Sommar, J., Lin, C.J., Feng, X., 2015a. Mercury vapor air–surface exchange measured by
439 collocated micrometeorological and enclosure methods – Part II: Bias and uncertainty analysis.
440 Atmos. Chem. Phys. 15, 5359-5376. 10.5194/acp-15-5359-2015

441 Zhu, W., Sommar, J., Lin, C.J., Feng, X., 2015b. Mercury vapor air–surface exchange measured by
442 collocated micrometeorological and enclosure methods – Part I: Data comparability and
443 method characteristics. Atmos. Chem. Phys. 15, 685-702. 10.5194/acp-15-685-2015

444

445